Functional characterization of human duodenal cytochrome *b* (Cybrd1): Redox properties in relation to iron and ascorbate metabolism

Jonathan S. Oakhill [a], Sophie J. Marritt [c], Elena Garcia Gareta [a],
Richard Cammack [b,*], Andrew T. McKie [a]

[a] *Nutritional Sciences Research Division, School of Biomedical and Health Sciences, King's College London, London, SE1 9NH, UK*
[b] *Pharmaceutical Sciences Research Division, School of Biomedical and Health Sciences, King's College London, London, SE1 9NH, UK*
[c] *Centre for Metalloprotein Spectroscopy and Chemistry, School of Chemical Sciences and Pharmacy, University of East Anglia, Norwich, NR4 7TJ, UK*

Abstract

Duodenal cytochrome *b* (*Dcytb or Cybrd1*) is an iron-regulated protein, highly expressed in the duodenal brush border membrane. It has ferric reductase activity and is believed to play a physiological role in dietary iron absorption. Its sequence identifies it as a member of the cytochrome b_{561} family. A His-tagged construct of human Dcytb was expressed in insect Sf9 cells and purified. Yields of protein were increased by supplementation of the cells with 5-aminolevulinic acid to stimulate heme biosynthesis. Quantitative analysis of the recombinant Dcytb indicated two heme groups per monomer. Site-directed mutagenesis of any of the four conserved histidine residues (His 50, 86, 120 and 159) to alanine resulted in much diminished levels of heme in the purified Dcytb, while mutation of the non-conserved histidine 33 had no effect on the heme content. This indicates that those conserved histidines are heme ligands, and that the protein cannot stably bind heme if any of them is absent. Recombinant Dcytb was reduced by ascorbate under anaerobic conditions, the extent of reduction being 67% of that produced by dithionite. It was readily reoxidized by ferricyanide. EPR spectroscopy showed signals from low-spin ferriheme, consistent with bis-histidine coordination. These comprised a signal at $g_{max} = 3.7$ corresponding to a highly anisotropic species, and another at $g_{max} = 3.18$; these species are similar to those observed in other cytochromes of the b_{561} family, and were reducible by ascorbate. In addition another signal was observed in some preparations at $g_{max} = 2.95$, but this was unreactive with ascorbate. Redox titrations indicated an average midpoint potential for the hemes in Dcytb of $+80$ mV ± 30 mV; the data are consistent with either two hemes at the same potential, or differing in potential by up to 60 mV. These results indicate that Dcytb is similar to the ascorbate-reducible cytochrome b_{561} of the adrenal chromaffin granule, though with some differences in midpoint potentials of the hemes.
© 2008 Elsevier B.V. All rights reserved.

Keywords: Duodenal cytochrome *b* (Dcytb); Iron; Heme coordination; Electron paramagnetic resonance spectroscopy (EPR spectroscopy); Magnetic circular dichroism-compatible optically-transparent thin-layer electrochemistry (MOTTLE)

1. Introduction

Uptake of dietary non-heme iron through the duodenal brush border membrane is one of the principal routes for assimilation of this essential element. At least 4 proteins, DMT1, Dcytb, ferroportin and hephaestin, have been implicated in the process (for a review read Anderson and Frazer [1]). The divalent cation transporter, DMT1 (also known as Nramp2, gene name Slc11a2), is believed to be responsible for initial uptake of iron from the duodenal lumen into the cells of the apical brush border membrane. DMT1 is specific for iron in its ferrous (Fe^{2+}) form, and since iron exists predominantly in its oxidized ferric (Fe^{3+}) form under the physiological conditions of the lumen [2], it should be reduced

prior to transport. Duodenal cytochrome b (Dcytb or *cybrd1*) fulfills many of the functional, positional and regulatory requirements for the ferric reductase. It is located in the brush border membrane, and there is evidence that it can function in reduction of ferric iron. In mice, Dcytb mRNA was shown to be strongly induced by iron deficiency, hypoxia and chronic and hemolytic anemias, all conditions in which iron absorption is increased [3]. In the duodenal wall, the site of highest iron-transporting activity is below the villus tip [4], and *in situ* hybridization showed Dcytb mRNA to be present almost exclusively in mature enterocytes at the villus tip, nearest to the intestinal lumen. Immunocytochemistry showed that the protein was located maximally in the apical membrane. The ability of Dcytb to catalyse the reduction of ferric to ferrous iron complexes at the cell surface was demonstrated by over-expression of the protein in cultured cell lines derived from intestinal cells and also in *Xenopus* oocytes [5]. Dcytb may have a broader role in cellular redox mechanisms; it is expressed in many tissues. In humans it is expressed in erythrocyte membranes, where it may contribute to reduction of extracellular dehydroascorbate. In mice, by contrast, the protein is only expressed in erythroblasts and is absent from mature erythrocytes [6].

The primary structure of Dcytb indicates that it is distinct from ferric reductases previously characterized in yeast [7,6], plants [8,9] and bacteria [10,11] and from STEAP3 of hematopoietic tissues [12]. Instead, Dcytb shares extensive structural homology (over 40% identity over the whole length) with cytochromes b_{561}, a class of proteins that transfer electrons from ascorbate across membranes, such as that of the adrenal chromaffin granule [13]. A topology model for cytochrome b_{561} [14,15,16] predicts an alpha-helical bundle with six putative transmembrane domains, four of which (II, III, IV and V) contain a single histidine heme-ligating residue. These residues are appropriately located to form two heme iron coordination complexes, located near the two surfaces of the membrane. Biochemical evidence implicating two of these residues, His86 and His159, as heme iron coordinating ligands has come from their individual site-directed mutation in recombinant cytochrome b_{561} expressed using a yeast system; each mutation resulted in the near elimination of a detectable difference heme spectrum despite protein expression levels comparable to that of wild-type [17]. The model was developed further by Okuyama et al. [18] following the recognition of two fully conserved sequences as potential substrate-binding domains. The first ([68]ALLVYRV[74]) is located at the extra-vesicular end of alpha-helix II, and in conjunction with Lys83 forms an ascorbate recognition/binding site [17], while the second ([119]SLHSW[123]) is thought to adopt an intra-vesicular location between helices II and III, forming another ascorbate or dehydroascorbate-binding site. This has led to a current mechanistic theory whereby the two heme iron centres undergo redox cycling to provide a conduit for electrons passing across the vesicle membrane, from an ascorbate donor to the ascorbyl radical acceptor.

It is likely that many inferences relating to cytochrome b_{561} are also applicable to Dcytb. The hydropathy profile of Dcytb indicates that it too forms six alpha-helical transmembrane domains, while sequence alignments indicate that the putative substrate-binding sites in cytochrome b_{561} are at least partially

conserved [5]. The proposal that ascorbate acts as the intracellular electron donor for Dcytb is supported by *in vivo* measurements that showed an increase in duodenal ascorbate levels in mice, induced to iron deficiency by feeding on an iron-depleted diet, hypoxia or genetic hypotransferrinemia [19]. Elevated duodenal and plasma ascorbate levels have also been associated with increased duodenal ferric reductase activity in iron-deficient human subjects [20]. Moreover, Su and Asard [6] have shown that in $\Delta fre1 \Delta fre2$ mutant yeast cells, in which the loss of endogenous ferric reductases can be complemented by transformation with the Dcytb gene, the surface ferric reductase activity is markedly increased when the transformed cells are grown on media containing the ascorbate precursor L-galactono-γ-lactone. A recent preliminary report on a canine kidney cell line showed that Dcytb enhanced the reduction of both Fe^{3+} and Cu^{2+} complexes in an ascorbate-dependent manner [21].

Apart from the inferences from sequences, information on the physical properties of Dcytb is very limited. In this study our aims were the determination of the presence and number of hemes, the identification of residues that bind heme, and the measurement of its oxidation-reduction properties. Preliminary attempts to express the protein in sufficient quantities for protein characterization by using a yeast system were unsuccessful, but finally sufficient quantities of the protein were obtained using a baculovirus-mediated expression system.

2. Materials and methods

2.1. Materials

The baculovirus transfer plasmid pTriEx-1.1, BacVector-3000 triple cut virus DNA, Sf9 insect cells, media and Bacplaque agarose were obtained from Novagen. TOP10 One Shot *Escherichia coli* was from Invitrogen. QuikChange site-directed mutagenesis kit was from Stratagene. Dodecyl-β-D-maltoside (DDM) and Elugent were from Calbiochem. Immunopure Goat anti-rabbit IgG-HRP conjugate and detergent compatible BCA assay kits, were obtained from Pierce. Chromatographic columns and Western blotting materials were from Amersham Biosciences. Centriprep and Centricon concentrators were from Millipore. All other materials were obtained from Sigma or Merck.

2.2. Preparation of recombinant baculovirus and site-directed mutagenesis

Human Dcytb cDNA was amplified by PCR techniques, introduced into pTriEx-1.1 baculovirus transfer vector to enable addition of a C-terminal histidine tag, and used to transform *E. coli* TOP10 cells. Plasmid DNA was extracted from a single carbenicillin-resistant colony, screened by direct sequencing and co-transfected into Sf9 cells with BacVector-3000 triple cut virus DNA using the manufacturer's recommended protocols. Positive recombinant baculovirus plaques were identified by Neutral Red staining, followed by propagation and direct sequencing. Virus titres were calculated using end point dilution assays, prior to expression studies.

Point mutations H33A, H50A, H86A, H120A and H159A were incorporated individually into the pTriEx-Dcytb transfer plasmid using the QuikChange kit, with successful inclusion of each verified by direct sequencing. Baculovirus stocks were generated as described above.

2.3. Insect cell cultures and Dcytb expression

Sf9 insect cells were grown in suspension cultures (28 °C, 150 rpm) for baculovirus propagation or attached monolayers (28 °C) for transfection. Expression medium was supplemented with 61 mg/l penicillin and 133 mg/l streptomycin.

For Dcytb (wild-type and mutant) expression, recombinant baculovirus was added at a multiplicity of infection (MOI) of 5–10 pfu/cell to 200 ml suspension cultures of Sf9 cells in logarithmic growth phase. Cells were incubated at 28 °C, 150 rpm and harvested five days post-infection by centrifugation at 3000 $\times g$, 4 °C for 10 min.

The 5-aminolevulinic acid (ALA) supplementation study was carried out on a 300 ml culture of Sf9 cells in logarithmic growth phase that was divided into 6×50 ml cultures. Five of these cultures were induced to express wild-type Dcytb as described above, while the other was infected at identical MOI with a baculovirus stock known to result in the expression of a non-heme, integral membrane protein. Cultures containing Dcytb-expressing cells were supplemented 24 h post-infection with ALA to final concentrations from 0–1.0 mM, while the non-hemoprotein expressing culture was supplemented 24 h post-infection with ALA to a final concentration of 1.0 mM.

2.4. Preparation of insect cell microsomal membranes

Harvested cell pellets were subjected to repeated freeze–thaw cycles. Subsequently, all membrane preparation steps were carried out at 4 °C, using ice-cold buffers. Cells were resuspended in one-tenth of the culture volume of 50 mM HEPES pH7.4, 250 mM NaCl, 30 mM imidazole (buffer A) supplemented with protease inhibitors: 1 mM AEBSF, 1 μM bestatin, 1 μM leupeptin, 1 μM pepstatin A, 100 μM E-64 and 2 μM phosphoramidon. Cells were lysed by 3×10 s low-intensity sonication pulses in a sonicator bath and heavy membrane fragments were pelleted by centrifugation at 2000 $\times g$ for 10 min. The supernatant was removed and microsomal membranes were recovered by centrifugation at 70,000 $\times g$ for 1 h in a Beckman Ti45 rotor. Pellets were washed with buffer A, prior to resuspension in one-tenth of the culture volume of buffer A plus protease inhibitor cocktail. Elugent was added dropwise with stirring to a final concentration of 2% (v/v). Membrane proteins were extracted using a magnetic stirrer at low revolutions for 1 h, and insolubilized material was pelleted by centrifugation at 100,000 $\times g$ for 1 h.

2.5. Immobilized metal affinity chromatography and sample preparation

All flow rates were maintained at 1 ml/min. Solubilized membrane proteins were loaded onto a column containing Ni-nitrilotriacetate (NTA) agarose, equilibrated with 10 column volumes of buffer A, 2% Elugent. The column was washed with 15 column volumes of buffer A, 0.05% DDM to remove unbound proteins, and to perform a detergent exchange. Bound proteins were then eluted with 10 column volumes of buffer A, 0.05% DDM supplemented with elevated imidazole concentrations, and collected in 1 ml fractions. Fractions containing Dcytb were concentrated using Centricon or Centriprep YM-50 concentrators at 3000 $\times g$, 4 °C. Residual imidazole was removed by dialysis against three changes of buffer A, 0.05% DDM at 4 °C, using a 10 kDa molecular weight cut-off dialysis membrane. Dialysis buffer was adjusted to pH7.0 for potentiometric titrations. Protein concentrations were determined using a detergent compatible BCA assay kit with bovine serum albumin as a standard.

2.6. Protein analysis

Standard techniques were used for resolving fractions on 12% SDS-PAGE gels [22]. 20 μl samples were diluted in an equal volume of Laemmli sample buffer at room temperature prior to electrophoresis at a constant 120 V. For Western blotting and N-terminal sequencing, fractions were then electroblotted overnight onto nitrocellulose paper at a constant 15 V, 4 °C. Western blots were developed using the ECL detection system, according to manufacturer's protocols. Briefly, active sites on the nitrocellulose paper were blocked for 1 h with PBS + 1% (w/v) powdered milk. Blots were then probed with rabbit anti-Dcytb antibody (1:250 dilution in PBS) for 1 h, followed by 4×5 min washes with PBS. Following incubation for 30 min with secondary antibody (goat anti-rabbit IgG-HRP, 1:40,000 dilution in PBS) and 4×5 min washes, blots were soaked in ECL developing solution for 5 min. Immunoreactive bands were visualized by autoradiography on Fuji X-ray film. N-terminal sequencing was conducted on an Applied Biosystems 473A protein sequencer.

To visualize hemoproteins following electrophoresis, fractions containing Dcytb were resolved according to the protocol previously recommended [23], using 0.1% lithium dodecyl sulfate (LDS) in the sample and running buffers

instead of SDS. Electrophoresis was conducted at a constant 90 V, 4 °C for 3 h. Staining was performed as previously described [24], based on the heme-associated, peroxidase-mediated formation of a blue precipitate from 3,3′-5,5′-tetramethylbenzidine.

2.7. Heme content analysis

Heme content of Dcytb samples was analyzed using the pyridine hemochromogen method as described previously [25]. The ferricyanide-oxidized spectrum was subtracted from the dithionite-reduced spectrum and heme b content was calculated using an extinction coefficient difference (556 nm–540 nm) of 24 mM^{-1} cm^{-1}.

2.8. Absorbance spectroscopy

200 μl samples were fully oxidized with addition of a small amount of ferricyanide and subjected to UV–visible absorbance spectroscopy at room temperature on a Synergy HT multi-detection microplate reader (Bio-Tek), using sample buffer as a blank. Samples were then fully reduced by the addition of sodium dithionite, and the absorption was measured over the same wavelength range. Difference spectra were obtained by subtracting the oxidized spectrum from the dithionite-reduced spectrum. For ascorbate reduction, Dcytb samples (0.1 mg/ml) were stirred under nitrogen for 1 h on ice. Measurements were performed with constant stirring in a stoppered self-masking cell under nitrogen flow. 50 μM ferricyanide was added until the sample was fully oxidized, as determined by stabilization of the 414 nm peak. 10 μl aliquots of 100 mM ascorbate in buffer A, pH7.5 were then added sequentially, with absorbance between 380 and 600 nm recorded 2 min after each addition. Once the spectrum had displayed maximal ascorbate reduction a few grains of sodium dithionite were added to fully reduce the sample.

2.9. EPR spectroscopy

Recombinant Dcytb was extracted, purified and concentrated to 70 μM as described above. Samples were frozen in liquid nitrogen prior to EPR analysis. Spectra were recorded at X-band continuous-wave mode, on a Bruker Elexsys E580 spectrometer or ESP300 spectrometer with an ER4122 Super-High-Q Cavity and an Oxford Instruments ESR900 helium flow cryostat.

2.10. Potentiometric titrations

Optically monitored potentiometric titrations were carried out in a 1 mm path-length quartz cuvette designed to perform magnetic circular dichroism with *in situ* potentiometric control (MOTTLE cell) [26]. Briefly, the cuvette was fitted with a gold mini-grid working electrode (60% optical transmission), and coated with cystamine prior to use. A platinum wire formed the counter electrode, and a silver chloride coated silver wire the reference electrode. Before sealing the cuvette cell with a rubber gasket, the reference electrode was calibrated by cyclic voltammetry of 100 μM potassium ferricyanide solution in 50 mM HEPES, 250 mM NaCl, pH7 buffer-electrolyte.

Dcytb samples were stirred under argon for 1 h on ice. A cocktail of mediators was added to a final concentration of 40 μM for each mediator: tetramethylphenylene diamine (240 mV vs. SHE), ruthenium hexamine chloride (201 mV), trimethylhydroquinone (100 mV), 5-hydroxynaphthoquinone (45 mV), duroquinone (7 mV), menadione (−80 mV), anthraquinone-2,6-disulfonate (−185 mV), anthraquinone-2-sulfonate (−225 mV), 5 μM benzyl viologen (−368 mV) and sulfonyl viologen (−390 mV). For the potential window investigated here the mediator cocktail showed negligible contribution to the electronic absorption spectrum. The spectroelectrochemical cell, flushed with argon gas, was loaded with 100 μl Dcytb (at a final concentration of 100 μM)-mediator solution and positioned inside a JASCO V-550 UV–visible spectrophotometer. This was connected to an Autolab PGSTAT 12 potentiostat controlled by GPES software.

A cyclic voltammogram was recorded to check the cell response and the integrity of the electrode connections. The desired potential was then applied to the sample and the approach to equilibrium monitored by the decrease in current magnitude to a negligible value and stabilization of the electronic absorbance at

560 nm. Equilibration typically took 20–30 min to achieve and the UV–visible absorption spectrum of the sample was then recorded. The potentiostat was set onto galvanostat mode to define the potential of the solution immediately after each spectrum had been recorded. The set and read-back potentials were typically within 30 mV of each other unless in a region of potential coinciding with a gap in the mediator potential range.

3. Results

3.1. Baculovirus-mediated Dcytb expression

Dcytb protein was localised exclusively to the membrane fraction, as indicated by a 30 kDa immunoreactive band in a Western blot of crude membrane extracts. (Fig. 1B, lane 2). Optimal yields of the cytochrome were obtained five days post-infection using a MOI value of 5. From a selection of detergent conditions tested, 2% Elugent provided the highest recovery rate of Dcytb from membrane preparations (data not shown). Dcytb could be isolated from microsomal membranes to approximately 90% purity using Ni^{2+}-NTA chromatography, as assessed by densitometric analysis of the Coomassie stained gels. We found that by employing a stringent primary elution of 150 mM imidazole we were able to remove the majority of contaminating proteins with only minor losses of recombinant protein (Fig. 1A and B, lanes 4 and 5).

Although N-terminal sequencing verified that the protein forming the major band at 30 kDa was Dcytb, two accompanying bands were also evident in 500 mM imidazole elution fractions, and both were immunoreactive to anti-Dcytb antibody (Fig. 1B, lane 5), suggesting the formation of Dcytb homo-dimers and -trimers. These complexes could be disrupted completely by heating samples at 100 °C for 5 min prior to electrophoresis, after which a single band slightly below 30 kDa was visualized (Fig. 1B, lane 6). The slightly higher electrophoretic mobility of the heated sample may represent monomeric Dcytb in a fully denatured form, or Dcytb lacking heme cofactors. All three immunoreactive bands could be eliminated
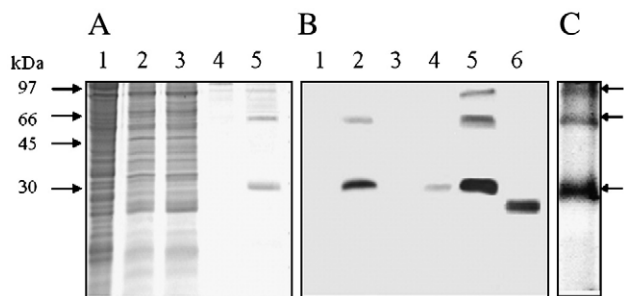

Fig. 1. Dcytb content of fractions collected during expression, extraction and purification protocols. Fractions were resolved by 12% SDS-PAGE, followed by either Coomassie staining (A), or transfer to nitrocellulose membrane and Western blotting with anti-Dcytb antibody (B). In both panels, lanes 1 and 2 respectively: Sf9 cell soluble and total membrane fractions; lane 3: Ni^{2+}-NTA column flow-through; lane 4: 150 mM imidazole elution; lane 5: 500 mM imidazole elution. (B) Lane 6: 500 mM imidazole elution fraction boiled for 5 min. Broad range molecular weight markers are shown on the left-hand side. (C) In-gel heme stain of 500 mM imidazole elution fraction containing holo-Dcytb. The membrane preparation used was collected from Dcytb-expressing insect cells, grown in medium which was supplemented with 1 mM ALA 24 h after baculovirus infection.
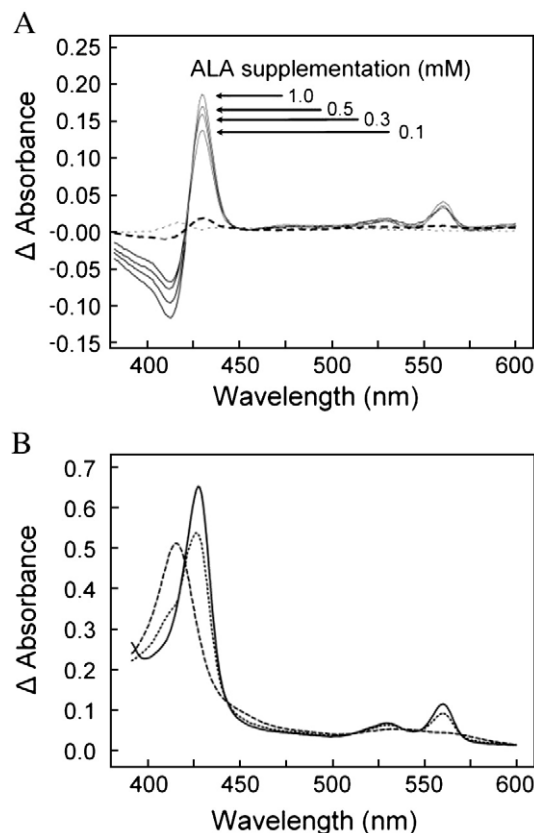

Fig. 2. UV–visible spectroscopy. (A) ALA supplementation of insect cell medium significantly increased the proportion of holo-Dcytb recovered. Reduced-minus-oxidized difference spectra were recorded from crude membrane fractions prepared from Sf9 cells expressing Dcytb without ALA supplementation (broken line), or with varying concentrations of ALA supplementation as noted. These are compared to the difference spectrum of a crude membrane preparation from Sf9 cells expressing a non-heme, integral membrane protein in the presence of 1 mM ALA (dotted line). All preparations were adjusted to 2 mg/ml total protein content prior to analysis. (B) Absorbance spectra of purified Dcytb in the UV–visible wavelength range following ferricyanide oxidation (broken line), dithionite reduction (solid line) or 15 mM (final concentration) ascorbate partial reduction (dotted line). Each spectrum was recorded under anaerobic conditions as described in Materials and methods.

by pre-incubation of the anti-Dcytb antibody with the peptide used to raise the antibody (not shown). Dcytb was consistently recovered in purified preparations at yields of 3–4 mg/l cell culture; the inclusion of 0.05% DDM enabled us to concentrate preparations to 6 mg/ml on 30 kDa molecular weight cut-off membranes without significant accumulation of surfactant.

3.2. ALA supplementation increases heme incorporation into Dcytb

Despite the high Dcytb concentrations achieved, initially it was clear from the absence of a distinct heme spectrum that the majority of the protein was present in the apo-form. As was shown in a previous study on recombinant adrenal cytochrome b_{561} [27], supplementation of the medium with ALA (a precursor in the heme biosynthetic pathway), added 24 h post-infection, greatly enhanced the heme content of Dcytb in insect cells. This was observed as it increased the peak amplitudes in

the difference spectra of microsomal membrane preparations (Fig. 2A). Comparisons with similar preparations from Sf9 cells induced to express a non-heme, integral membrane protein in ALA supplemented media indicated that the spectra obtained were direct measurements of Dcytb and not an endogenous hemoprotein. Heme loading increased with ALA supplementation up to 1 mM, above which a significant reduction in Dcytb expression was observed. At this level of ALA supplementation heme content analysis, coupled to a detergent compatible BCA assay to estimate protein concentration, indicated that an average of 1.67 heme b was present per Dcytb monomer. In-gel heme staining of heme-loaded Dcytb fractions resolved by LDS-PAGE produced a similar band profile to that obtained by Western blotting (Fig. 1C), with a major band at 30 kDa and two other bands at approximately 60 kDa and 90 kDa.

UV–visible absorption spectroscopy of oxidized Dcytb indicated the presence of a characteristic Soret band at 413 nm. This shifted to 424 nm after full reduction by dithionite, and was accompanied by the detection of a single α band at 560 nm, and a smaller β band at 529 nm. There is a slight asymmetry in the lower-wavelength side of the α band of the partially-reduced cytochrome, as observed in the spectrum of cytochrome b_{561} by Kamensky et al. [28] (see Fig. 5A); this may reflect the presence of two hemes with somewhat different absorption spectra. The difference spectra for Dcytb displayed in Fig. 2A are characteristic of a b-type cytochrome, as expected.

Dcytb was reducible by ascorbate under anaerobic conditions (Fig. 2B), with the proportion of reduced cytochrome increasing in a concentration dependent manner up to 15 mM ascorbate, above which no further reduction was observed. The relative absorbance of the difference spectrum at 560 nm (α band) indicated that Dcytb was 67% reducible by ascorbate in comparison to dithionite reduction.

3.3. EPR spectroscopic measurements

Recombinant Dcytb in the oxidized state showed an EPR spectrum at temperatures around 12K, typical of low-spin ferric heme. Fig. 3A shows a sample from the same batch as that used for redox titrations. The $g_z=3.7$, 3.18 components are similar to those observed in CG cytochrome b_{562} from adrenal chromaffin granules [29,28]. This spectrum is consistent with the presence of two hemes in the cytochrome. The highly anisotropic $g_{max}=3.7$ feature is from a more rapidly-relaxing species that was not perceptible at temperatures above 12 K (Fig. 3Aa and b). Signals at $g>3.3$ are characteristic of the highly anisotropic low-spin form seen in some other bis-histidine heme compounds and proteins [30].

Preparations of Dcytb often also displayed a signal at $g_1=2.95$, $g_2=2.25$ in addition to the signal at $g_{max}=3.18$. In extreme cases the $g_{max}=2.95$ feature was very prominent, and the signal at $g_{max}=3.7$ was undetectable (Fig. 3Bd). The $g_{max}=3.7$,
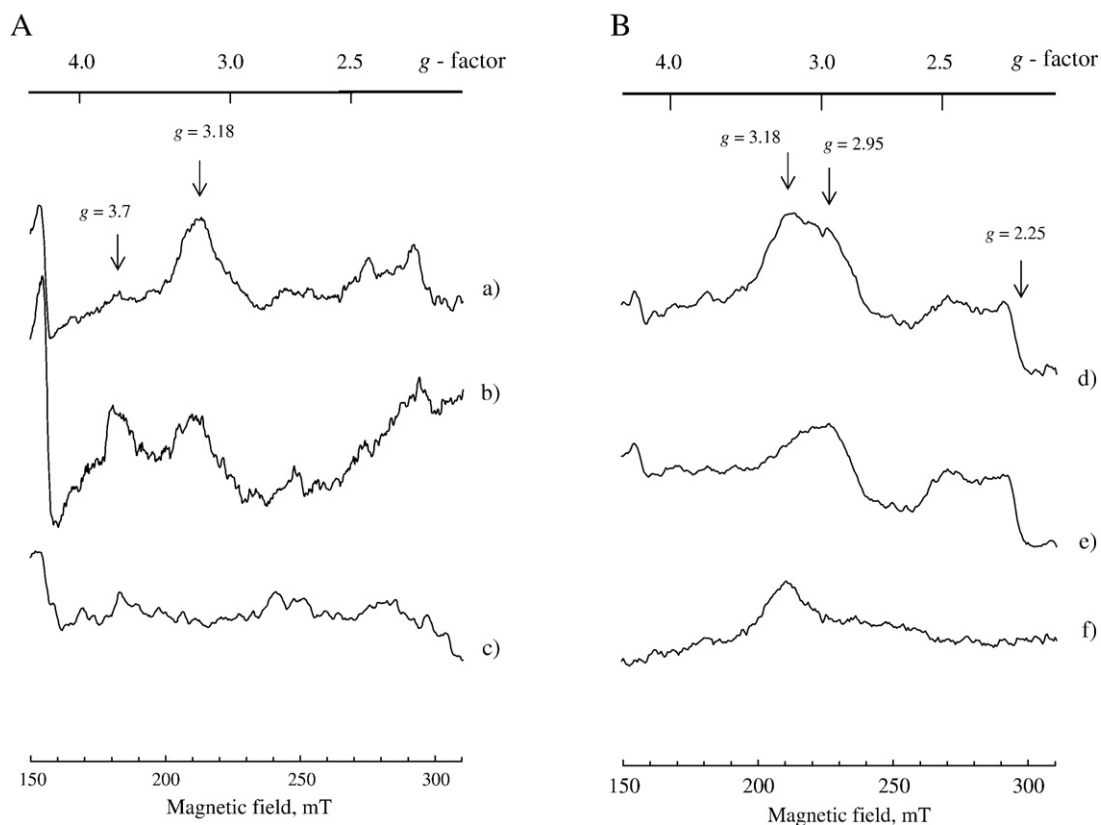

Fig. 3. (A) EPR spectra of purified recombinant Dcytb after metal affinity chromatography, a) recorded at 17 K; b) recorded at 9.5 K; c) reduced with 10 mM ascorbate for 2 min, recorded at 9.5 K. Conditions of measurement were: microwave power 20 mW, frequency 9.40 GHz, modulation amplitude 1 mT. (B) EPR spectrum of recombinant Dcytb, prepared by detergent extraction without sonication d) recorded at 12 K; e) reduced with 5 mM ascorbate, 12 K; f) difference, oxidized minus ascorbate-reduced. Conditions as for (A), except microwave frequency 9.38 GHz.
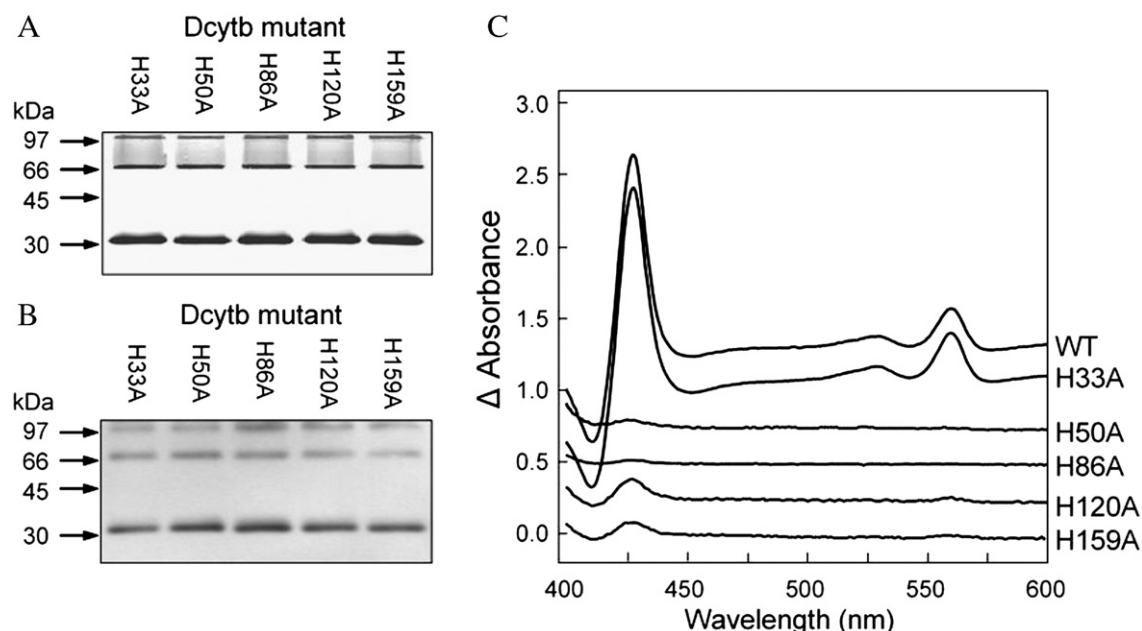
Fig. 4. Expression and difference spectra of Dcytb mutants. Mutated Dcytb was prepared as described for wild-type in Materials and methods and resolved by 12% SDS-PAGE, followed by (A) Coomassie staining, or (B) transfer to nitrocellulose membrane and Western blotting with anti-Dcytb antibody. (C) Reduced-minus-oxidized difference spectra of mutated vs. wild-type Dcytb preparations. Samples were adjusted to 0.5 mg/ml with 50 mM HEPES pH7.4, 250 mM NaCl, 0.05% DDM prior to spectroscopic analysis of 200 µl in a 96 well plate reader. Results shown are representative of three individual preparations of each mutant.

3.18 and 2.95 features could be distinguished by their reducibility by ascorbate. In the sample shown in Fig. 3A, the EPR signal at $g_{max}=3.18$ disappeared, while the signal at $g_{max}=3.7$ was substantially decreased (Fig. 3Ac). Fig. 3B shows spectra of another sample, prepared by a method that involved detergent extraction without sonication. The $g_{max}=3.7$ signal in this preparation was relatively low. On reduction by ascorbate (Fig. 3Be), the $g_{max}=3.18$ signal was reduced, as seen in the difference spectrum (Fig. 3Bf) but the $g_{max}=2.95$ signal was apparently unchanged. This indicates that the $g_{max}=2.95$ species either has a lower redox potential than the other hemes, or is unreactive with ascorbate.

3.4. Sequence-directed mutagenesis

To investigate the identity of the heme-ligating His residues indicated by EPR analysis, we generated site-directed mutants of candidates from a sequence alignment with cytochromes b_{561} [5]. Expression levels of mutants H33A, H50A, H86A, H120A and H159A by Sf9 cells in 1.0 mM ALA supplemented media
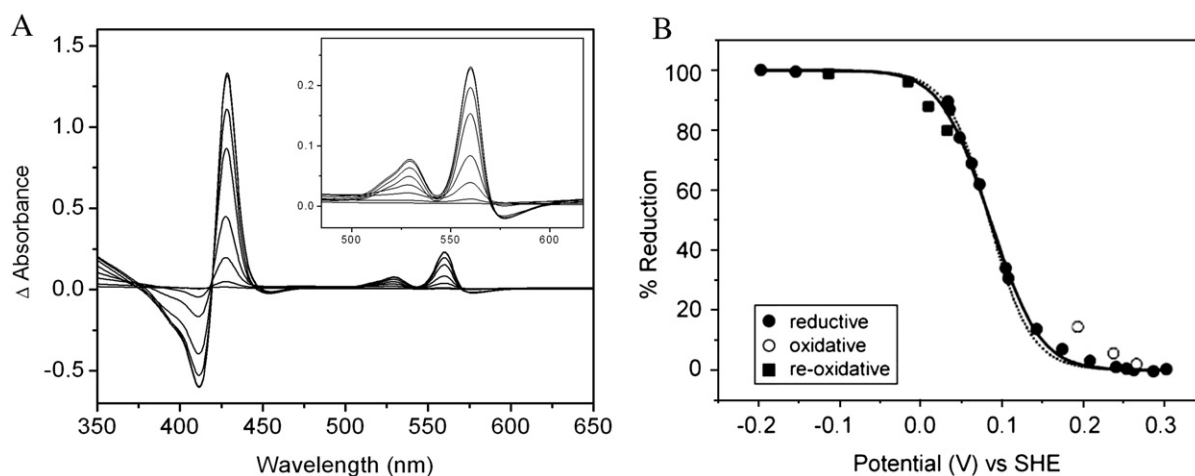

Fig. 5. Dcytb potentiometric titration. A 100 µM purified Dcytb sample was mixed with various potential mediators as described in Materials and methods and redox status was monitored in a MOTTLE cell at pH7.0 under anaerobic conditions. (A) Difference spectra at equilibrated potentials between −197 mV and +241 mV during the reductive titration, showing a normal reduction profile. Inset is a magnified view of the apha- and beta-bands. (B) Redox titration profile plotting % reduction, as measured by absorbance at 560 nm–572 nm, against potential vs. SHE (standard hydrogen electrode). Fits to the Nernst equation; (─) for two reduction potentials of $E_m=58$ mV and 108 mV (coefficient of determination $r^2=0.9965$), and (----) for one reduction potential of $E_m=83$ mV ($r^2=0.9944$).

were verified by SDS-PAGE and Western blotting (Fig. 4A and B). In each case the mutated protein was located exclusively to the membrane fraction and could be extracted in similar yields to the wild-type protein. The H50A and H120A mutants appeared to be properly processed and targeted in Sf9 cells, in contrast to the corresponding mutants of cytochrome b_{561} when expressed in yeast [17]. The effect on heme binding conferred by each mutation was assessed by comparing the difference spectra of 0.5 mg/ml samples of the Dcytb mutants to the wild-type protein. His33 was mutated as a control; it is not conserved between Dcytb and cytochrome b_{561} but is proposed to be positioned within transmembrane alpha-helix I. The difference spectrum for the mutant in the non-conserved His33 was similar to the wild-type in terms of band position and amplitude, suggesting that the mutation did not significantly affect the overall processing and folding of Dcytb. However each of the mutations of the other histidine residues resulted in a substantial, though not complete, loss of the heme spectrum.

3.5. Dcytb potentiometry

As the Dcytb sample was found to be slightly reduced prior to amperometry an initial oxidative poising was performed to record a fully oxidized UV–visible spectrum. A full reductive titration from +241 mV to −180 mV was performed at ambient temperature, followed by a partial re-oxidation. Fig. 5A shows the difference spectra (reduced minus oxidized) for the b hemes in Dcytb, equilibrated at various potentials during the reductive titration. Fig. 5B shows the titration profile for Dcytb, plotting % reduction as monitored by the increase in intensity of the α band at 560 nm. The absorbance difference 560 nm minus the 572 nm isosbestic point is plotted to correct for any baseline shifts and mediator contribution in this region of the spectra. The reduction profile shows a continuous sigmoid curve with no inflexion. It was possible to obtain a reasonable fit to the data with a single reversible one-electron Nernstian process with a reduction potential of +86 mV (solid line). A somewhat better fit could be obtained with two components, each at 50% intensity, with reduction potentials of +110 mV and +60 mV (dotted line). Resolution of the Nernst curves of two components is difficult if the difference in potential is less than 40 mV [31]. Similar cases of heme proteins with overlapping redox potentials have been described, such as chloroplast cytochrome b_6 [32].

By comparison, the potentials of the two hemes in CG cytb_{561} are somewhat more positive than those of Dcytb, and sufficiently separated to be fitted to two components. Apps et al. [33] fitted their redox data to potentials of 170 and 70 mV for the soluble protein, and 135 and 55 mV for the membrane-bound form.

4. Discussion

The duodenal enterocyte represents the major regulatory site controlling iron homeostasis in mammals. Dcytb has been shown to be a transmembrane protein, with ferric reductase activity, and to be expressed in the intestine. Both mRNA and protein are high regulated by iron status of the body, and the enzyme is thought to play an important role in absorption of dietary iron, at least in humans. However there are probably multiple pathways of iron reduction. Gunshin et al. [34] reported that Dcytb knockout mice, when grown either under normal or iron-limited conditions, did not become anemic and showed only a modest decrease in liver iron content. They concluded that Dcytb is not essential for intestinal iron uptake under the growth conditions used. This does not rule out a role of Dcytb in iron reduction however [35]. Mice of the strain used (129S6SvEx-Tac) have unusually high liver iron levels and do not become anemic when fed an iron-deficient diet, whereas other mouse strains and humans might be expected to do so [34,36]. On a normal diet there may be a significant non-enzymic reduction of iron by reducing compounds in the intestine. Moreover mice, unlike humans, are able to synthesize ascorbate and might secrete ascorbate into the gastrointestinal tract, so there would be no absolute requirement for a surface ferric reductase. Further work is needed on compensatory mechanisms of duodenal iron reduction and absorption.

The development of an expression system to address these questions is therefore timely. It complements those described for recombinant cytochrome b_{561}, expressed in Sf9 cells, P. pastoris [27] and S. cerevisiae [17].

4.1. The number of hemes per molecule

Heme content analyses of Dcytb derived from Sf9 cells growing in medium supplemented with ALA indicate that our preparations contained an average of ≈ 1.7 heme b per Dcytb monomer indicating that Dcytb is a di-heme protein. The EPR spectra are also consistent with the presence of two different hemes in equal concentrations. This is similar to data on CG cytochrome b_{561} which indicated a heme b: protein monomer ratio of 2:1 [27,29]. In addition, the Dcytb EPR spectrum at 12 K has similar features to those of cytochrome b_{561} recorded at 15 K [27–29]. The presence of two hemes with bis-histidine co-ordination is supported by the site-directed mutagenesis studies, in which the substitution of any of the identified four Dcytb histidine residues led to a loss of most, but not all, of the heme spectrum. The equivalent histidine residues are conserved in the cytochrome b_{561} sequence, and have been shown to be required for Fe^{3+} reductase activity [17], or following point mutation of lysosomal cytochrome b_{561} expressed in $\Delta fre1 \Delta fre2$ mutant yeast cells [6]. Substitution of the non-conserved His33 had negligible effect on heme binding, as was observed for mutation of the equivalent histidine in cytochrome b_{561}. Protein expression levels were unchanged in each case. Similar results were reported for CG cytochrome b_{561} [17,28]. These results indicate a cooperative binding of hemes, such that binding of heme to either site facilitates the insertion of heme into the other, or stabilizes it once inserted. Studies of synthetic four-helix protein maquettes containing pairs of hemes with bis-histidyl coordination have shown that, in some cases, loss of one histidine destabilizes the structure of the whole [37]. The calculated Dcytb extinction coefficients in our preparations were approximately 228 mM^{-1} cm^{-1} (428 nm–411 nm) and 29 mM^{-1} cm^{-1} (560 nm–575 nm), although these are minimal

estimates due to partial heme loading. The values are slightly lower than representative values for cytochrome b_{561} from bovine adrenal glands [29].

The samples prepared during this study had a tendency to form homo-dimeric and homo-trimeric Dcytb complexes, indicating some heterogeneity in the preparations (Figs. 1 and 4). Mammalian cytochrome b_{561} [38] and a plant homologue isolated from etiolated bean hypocotyls [39] were also reported to form aggregates in detergent solubilized extracts. It is unlikely that this oligomerization of recombinant Dcytb is due to non-specific interactions between histidine affinity tags since we and others have observed the effect in membrane extracts of mammalian cultured cells expressing Dcytb without an affinity tag (data not shown) and in murine duodenal lysates [34]. The physiological relevance of cytochrome b aggregation is unclear at the present time.

The EPR spectra of the recombinant Dcytb comprised differing amounts of three heme species, depending on the preparation, with $g_{max} = 3.7$, 3.18 and 2.95. The $g_{max} = 3.18$ species was always present, but the $g_{max} = 3.7$ and 2.95 signals appeared to represent alternative species. The most recent preparations, obtained by ultrasonic treatment and purified on the Ni-NTA column, showed a more prominent $g_{max} = 3.7$ signal (Fig. 3A), similar to those seen in other cytochromes of the b_{561} family [28]. In the classification of Walker [30, 40] this highly anisotropic signal represents a Type I heme, in which the imidazole planes of the coordinating histidines are orthogonal. Other preparations, such as the sample prepared by detergent extraction without sonication in Fig. 3B, showed a more prominent $g_{max} = 2.95$ signal which was associated with a second g-factor of 2.25. This represents a Type II heme, in which the imidazole rings are closer to parallel [30]. These data can be interpreted in terms of a structural modification of the protein, in which the $g_{max} = 3.7$ heme is converted from Type I to Type II. The reason for the change in coordination in Dcytb remains to be established. Such changes in conformation have been observed in CG cytochrome b_{561}, where the heme with $g_{max} = 3.1$ could be modified by treatment with ferricyanide at alkaline pH, giving a species with $g_{max} = 2.84$ [29]. Takeuchi et al. [16] also described a form of CG cytochrome b_{561}, obtained by treatment with a cysteine-modifying agent, in which the $g_{max} = 3.1$ species was converted to a form with $g_{max} = 2.94$. Interestingly, this form was not reducible by ascorbate.

4.2. On the function of Dcytb

The present study indicates that recombinant Dcytb contains two hemes that are at least partially ascorbate-reducible. In a static reduction experiment, 67% of the heme was reduced by ascorbate. The measured midpoint potentials of the hemes indicate that the ascorbyl radical/ascorbate couple at +320 mV [41,42] would not be sufficient to carry out the reduction. More likely it is the reducing couple which is dehydroascorbate/ ascorbate, which has a potential of +58 mV. Dehydroascorbate is unstable, being converted to 2,3-dioxogulonate, on a timescale of several minutes [43] which would drive the reduction further. In vivo, dehydroascorbate would be kept at very low levels by being rapidly re-reduced to ascorbate, for example by reaction with glutathione. The binding site for ascorbate in cytb_{561} is conserved in the sequence of Dcytb [5]. The hemes have the necessary reduction potential to transfer electrons to Fe^{3+}, and the protein is oxidized by ferricyanide. Nevertheless it is difficult to establish unequivocally from studies of the recombinant protein, that the sole physiological role of Dcytb is as a specific ascorbate-dependent Fe^{3+} reductase. Firstly, Dcytb has the capacity to reduce other electron acceptors such as tetrazolium [5]. Secondly, ascorbate and Fe^{3+} complexes will rapidly react with each other in free solution. Some support for ascorbate as the electron donor to Dcytb is the conservation of residues Arg70, Lys83, His86 and His159 which in b_{561} have been implicated in ascorbate-binding using diethyl pyrocarbonate modification studies [44] and site-directed mutagenesis [17]. In addition, the measured midpoint potential of +80 mV for purified Dcytb correlates well with that of the lower redox potential heme species of cytochrome b_{561} (+70 mV, [33]), which is proposed to act as the electron acceptor from cytoplasmic ascorbate [29]. The best functional evidence at present comes from the studies already mentioned, [6,19,20] which showed that expression of Dcytb in cell membranes enhanced the reduction of Fe^{3+} in an ascorbate-dependent manner.

In summary, this is the first report of the isolation of Dcytb, the protein which is most highly induced in the enterocyte during iron deprivation [3]. The data provide direct evidence that the cytochrome contains two heme groups per molecule and identify four critical histidine residues predicted to be involved in heme binding. In these respects, and in spectroscopic properties, Dcytb is similar to other cytochromes of the b_{561} family. We have measured the midpoint reduction potentials of the hemes, and shown that they are reducible by ascorbate indicating this as a likely intracellular electron donor.

References

[1] F.L. Crane, I.L. Sun, M.G. Clark, C. Grebing, H. Low, Transplasma-membrane redox systems in growth and development, Biochim. Biophys. Acta 811 (1985) 233–264.

[2] H. Gunshin, B. Mackenzie, U.V. Berger, Y. Gunshin, M.F. Romero, W.F. Boron, S. Nussberger, J.L. Gollan, M.A. Hediger, Cloning and characterization of a mammalian proton-coupled metal-ion transporter, Nature 388 (1997) 482–488.

[3] G.O. Latunde-Dada, C.D. Vulpe, G.J. Anderson, R.J. Simpson, A.T. McKie, Tissue-specific changes in iron metabolism genes in mice following phenylhydrazine-induced haemolysis, Biochim. Biophys. Acta— Mol. Basis Dis. 1690 (2004) 169–176.

[4] D.K. O'Riordan, P. Sharp, R.M. Sykes, S.K. Srai, O. Epstein, E.S. Debnam, Cellular mechanisms underlying the increased duodenal iron-

absorption in rats in response to phenylhydrazine-induced hemolytic-anemia, Euro. J. Clin. Investig. 25 (1995) 722–727.

[5] A.T. McKie, D. Barrow, G.O. Latunde-Dada, A. Rolfs, G. Sager, E. Mudaly, M. Mudaly, C. Richardson, D. Barlow, A. Bomford, T.J. Peters, K.B. Raja, S. Shirali, M.A. Hediger, F. Farzaneh, R.J. Simpson, An iron-regulated ferric reductase associated with the absorption of dietary iron, Science 291 (2001) 1755–1759.

[6] D. Su, H. Asard, Three mammalian cytochromes b(561) are ascorbate-dependent ferrireductases, Febs J. 273 (2006) 3722–3734.

[7] A. Dancis, D.G. Roman, G.J. Anderson, A.G. Hinnebusch, R.D. Klausner, Ferric reductase of *Saccharomyces cerevisiae* — molecular characterization, role in iron uptake, and transcriptional control by iron, Proc. Natl. Acad. Sci. U. S. A. 89 (1992) 3869–3873.

[8] N.J. Robinson, C.M. Procter, E.L. Connolly, M.L. Guerinot, A ferric-chelate reductase for iron uptake from soils, Nature 397 (1999) 694–697.

[9] A. Berczi, D. Su, H. Asard, An Arabidopsis cytochrome b561 with trans-membrane ferrireductase capability, FEBD Lett. 581 (2007) 1505–1508.

[10] M. Fontecave, J. Coves, J.L. Pierre, Ferric reductases or flavin reductases, Biometals 7 (1994) 3–8.

[11] M. Tsubaki, F. Takeuchi, N. Nakanishi, Cytochrome b561 protein family: expanding roles and versatile transmembrane electron transfer abilities as predicted by a new classification system and protein sequence motif analyses, BBA—Proteins Proteomics 1753 (2005) 174–190.

[12] R.S. Ohgami, D.R. Campagna, E.L. Greer, B. Antiochos, A. McDonald, J. Chen, J.J. Sharp, Y. Fujiwara, J.E. Barker, M.D. Fleming, Identification of a ferrireductase required for efficient transferrin-dependent iron uptake in erythroid cells, Nat. Genet. 37 (2005) 1264–1269.

[13] T. Takigami, F. Takeuchi, M. Nakagawa, T. Hase, M. Tsubaki, Stopped-flow analyses on the reaction of ascorbate with cytochrome b(561) purified from bovine chromaffin vesicle membranes, Biochemistry 42 (2003) 8110–8118.

[14] M.D. Degli Esposti, Y.A. Kamensky, A.M. Arutjunjan, A.A. Konstantinov, A Model for the molecular organization of cytochrome b-561 in chromaffin granule membranes, FEBS Lett. 254 (1989) 74–78.

[15] D. Bashtovyy, A. Berczi, H. Asard, T. Pali, Structure prediction for the di-heme cytochrome b(561) protein family, Protoplasma 221 (2003) 31–40.

[16] F. Takeuchi, H. Hori, M. Tsubaki, Selective perturbation of the intravesicular heme center of cytochrome b(561) by cysteinyl modification with 4,4'-dithiodipyridine, J. Biochem. 138 (2005) 751–762.

[17] A. Berczi, D. Su, M. Lakshminarasimhan, A. Vargas, H. Asard, Heterologous expression and site-directed mutagenesis of an ascorbate-reducible cytochrome b561, Arch. Biochem. Biophys. 443 (2005) 82–92.

[18] E. Okuyama, R. Yamamoto, Y. Ichikawa, M. Tsubaki, Structural basis for the electron transfer across the chromaffin vesicle membranes catalyzed by cytochrome b(561): analyses of cDNA nucleotide sequences and visible absorption spectra, Biochim. Biophys. Acta—Protein Struct. Molec. Enzym. 1383 (1998) 269–278.

[19] B. Atanasova, I.S. Mudway, A.H. Laftah, G.O. Latunde-Dada, A.T. McKie, T.J. Peters, K.N. Tzatchev, R.J. Simpson, Duodenal ascorbate levels are changed in mice with altered iron metabolism, J. Nutr. 134 (2004) 501–505.

[20] B.D. Atanasova, A.C.Y. Li, I. Bjarnason, K.N. Tzatchev, R.J. Simpson, Duodenal ascorbate and ferric reductase in human iron deficiency, Am. J. Clin. Nutr. 81 (2005) 130–133.

[21] S. Wyman, M. Shayeghi, R. Simpson, A. McKie, P. Sharp, Establishment of a stably transfected cell line to study the function of the ferric reductase Dcytb, Am. J. Hematol. 82 (2007) 584–584.

[22] U.K. Laemmli, Cleavage of structural proteins during assembly of the head of bacteriophage T4, Nature 227 (1970) 680–685.

[23] J.F. Sinclair, J.F. Healey, R. McAllister, H.L. Bonkowsky, P.R. Sinclair, Improved retention of heme with increased resolution of microsomal proteins in polyacrylamide-gel electrophoresis, Anal. Biochem. 114 (1981) 316–321.

[24] P.E. Thomas, D. Ryan, W. Levin, Improved staining procedure for detection of peroxidase-activity of cytochrome-p-450 on sodium dodecyl-sulfate polyacrylamide gels, Anal. Biochem. 75 (1976) 168–176.

[25] E.A. Berry, B.L. Trumpower, Simultaneous determination of hemes-a, hemes-b, and hemes-c from pyridine hemochrome spectra, Anal. Biochem. 161 (1987) 1–15.

[26] S.J. Marritt, J.H. van Wonderen, M.R. Cheesman, J.N. Butt, Magnetic circular dichroism of hemoproteins with in situ control of electrochemical potential: "MOTTLE", Anal. Biochem. 359 (2006) 79–83.

[27] W. Liu, Y. Kamensky, R. Kakkar, E. Foley, R.J. Kulmacz, G. Palmer, Purification and characterization of bovine adrenal cytochrome b(561) expressed in insect and yeast cell systems, Protein Expr. Purif. 40 (2005) 429–439.

[28] Y. Kamensky, W. Liu, A.L. Tsai, R.J. Kulmacz, G. Palmer, Axial ligation and stoichiometry of heme centers in adrenal cytochrome b(561), Biochemistry 46 (2007) 8647–8658.

[29] M. Tsubaki, M. Nakayama, E. Okuyama, Y. Ichikawa, H. Hori, Existence of two heme B centers in cytochrome b(561) from bovine adrenal chromaffin vesicles as revealed by a new purification procedure and EPR spectroscopy, J. Biol. Chem. 272 (1997) 23206–23210.

[30] F.A. Walker, Models of the bis-histidine-ligated electron-transferring cytochromes. Comparative geometric and electronic structure of low-spin ferro- and ferrihemes, Chem. Rev. 104 (2004) 589–615.

[31] R. Cammack, Redox states and potentials, in: G.C. Brown, C.E. Cooper (Eds.), Bioenergetics: a Practical Approach, IRL Press, Oxford, 1995, pp. 85–109.

[32] P.N. Furbacher, M.E. Girvin, W.A. Cramer, On the question of interheme electron-transfer in the chloroplast cytochrome-b6 in situ, Biochemistry 28 (1989) 8990–8998.

[33] D.K. Apps, M.D. Boisclair, F.S. Gavine, G.W. Pettigrew, Unusual redox behavior of cytochrome-b-561 from bovine chromaffin granule membranes, Biochim. Biophys. Acta 764 (1984) 8–16.

[34] H. Gunshin, C.N. Starr, C. DiRenzo, M.D. Fleming, J. Jin, E.L. Greer, V.M. Sellers, S.M. Galica, N.C. Andrews, Cybrd1 (duodenal cytochrome b) is not necessary for dietary iron absorption in mice, Blood 106 (2005) 2879–2883.

[35] D.M. Frazer, S.J. Wilkins, C.D. Vulpe, G.J. Anderson, The role of duodenal cytochrome b in intestinal iron absorption remains unclear, Blood 106 (2005) 4413–4413.

[36] Y. Ohira, S.L. Gill, Effects of dietary iron-deficiency on muscle-fiber characteristics and whole-body distribution of hemoglobin in mice, J. Nutr. 113 (1983) 1811–1818.

[37] B.M. Discher, D. Noy, J. Strzalka, S.X. Ye, C.C. Moser, J.D. Lear, J.K. Blasie, P.L. Dutton, Design of amphiphilic protein maquettes: controlling assembly, membrane insertion, and cofactor interactions, Biochemistry 44 (2005) 12329–12343.

[38] Y. Kamensky, R.J. Kulmacz, G. Palmer, Composition of the heme centers in chromaffin granule cytochrome b(561), Chromaffin Cell: Transmitter Biosynthesis, Storage, Release, Actions, and Informatics, 971, 2002, pp. 450–453.

[39] V. Preger, S. Scagliarini, P. Pupillo, P. Trost, Identification of an ascorbate-dependent cytochrome b of the tonoplast membrane sharing biochemical features with members of the cytochrome b561 family, Planta 220 (2005) 365–375.

[40] L.A. Yatsunyk, A. Dawson, M.D. Carducci, G.S. Nichol, F.A. Walker, Models of the cytochromes: crystal structures and EPR spectral characterization of low-spin bis-imidazole complexes of (OETPP)Fe-III having intermediate ligand plane dihedral angles, Inorg. Chem. 45 (2006) 5417–5428.

[41] W.M. Clark, The Oxidation-Reduction Potentials of Organic Systems, The Williams and Wilkins Company, 1960.

[42] P.W. Washko, R.W. Welch, K.R. Dhariwal, Y.H. Wang, M. Levine, Ascorbic acid and dehydroascorbic acid analyses in biological samples—Review, Anal. Biochem. 204 (1992) 1–14.

[43] G. Banhegyi, L. Braun, M. Csala, F. Puskas, J. Mandl, Ascorbate metabolism and its regulation in animals, Free Radic. Biol. Med. 23 (1997) 793–803.

[44] M. Tsubaki, K. Kobayashi, T. Ichise, F. Takeuchi, S. Tagawa, Diethyl pyrocarbonate modification abolishes fast electron accepting ability of cytochrome b(561) from ascorbate but does not influence electron donation to monodehydroascorbate radical: identification of the modification sites by mass spectrometric analysis, Biochemistry 39 (2000) 3276–3284.